



THE UNIVERSITY  
OF QUEENSLAND  
AUSTRALIA



JOHANN WOLFGANG GOETHE  
UNIVERSITÄT  
FRANKFURT AM MAIN

UCSF School of  
Medicine



# Relationships between *in vivo* skin permeability and regional variations in morphological and biophysical skin properties

Eman Abd<sup>1</sup>, Yousuf Mohammed<sup>1</sup>, Arne Naegel<sup>3</sup>, Jeffrey Grice<sup>1</sup>, Rebecca Wittum<sup>3</sup>, Michael Heisig<sup>3</sup>, Gabriel Wittum<sup>3</sup>, Howard Maibach<sup>4</sup>, Michael S. Roberts<sup>1,2</sup>

Therapeutics Research Centre, <sup>1</sup>UQ Diamantina Institute, Brisbane & <sup>2</sup>School of Pharmacy & Medical Sciences, UniSA, Adelaide, Australia, <sup>3</sup>Goethe-Centre for Scientific Computing, Goethe University, Frankfurt, Germany, <sup>4</sup>UCSF School of Medicine

**Purpose** Variability in skin properties between anatomical sites is likely to cause differences in topical bioavailability at different parts of the body. This must be considered when the *in vivo* site of application for a product (e.g. acyclovir applied to lips) differs from the site used for *in vivo* microdialysis studies (e.g. the thigh), or the anatomical site from which skin is obtained for *in vitro* permeation tests (IVPT) (e.g. the abdomen). Here, we characterized biophysical properties and skin morphology in 13 normal volunteers at 22 anatomical sites to provide parameters with which to refine 3D skin permeation models [1]. The overall aim was to predict the *in vivo* permeation of solutes at a specific anatomical site, based on IVPT data obtained using skin from a different body site.

## Methods

• *In vivo* skin morphology of 7 male and 6 female volunteers aged 20 - 40 yrs, with no evidence of skin disease, was imaged by reflectance confocal microscopy (RCM; Vivascope 1500, Lucid).

• Various anatomical sites studied: scalp, post-auricular, forehead, cheek, nose, lip, chin, chest, neck, abdomen, back, axillary, elbow, ventral and dorsal forearm, palm, back of hand, dorsal finger, thigh, calf, sole and toe.

• Skin layers and morphological features including the thicknesses of stratum corneum (SC), viable epidermis (VE), and papillary dermal (PD) regions, the depth and width of skin furrows, and the density and orifice sizes of hair follicles and eccrine sweat glands were identified in Z-stack images and measured with ImageJ software (NIH).

• Transepidermal water loss (TEWL) and skin hydration (SH) were measured non-invasively with an evaporimeter (AquaFlux, Biox Systems) and a Corneometer (Courage+Khazaka), respectively.

**Results 1.** The SC and VE thickness was greatest at anatomical sites subjected to the greatest friction (palm, elbow, finger, sole and toe), but there were no significant differences in the papillary dermal thickness between these and other sites (Fig. 1).

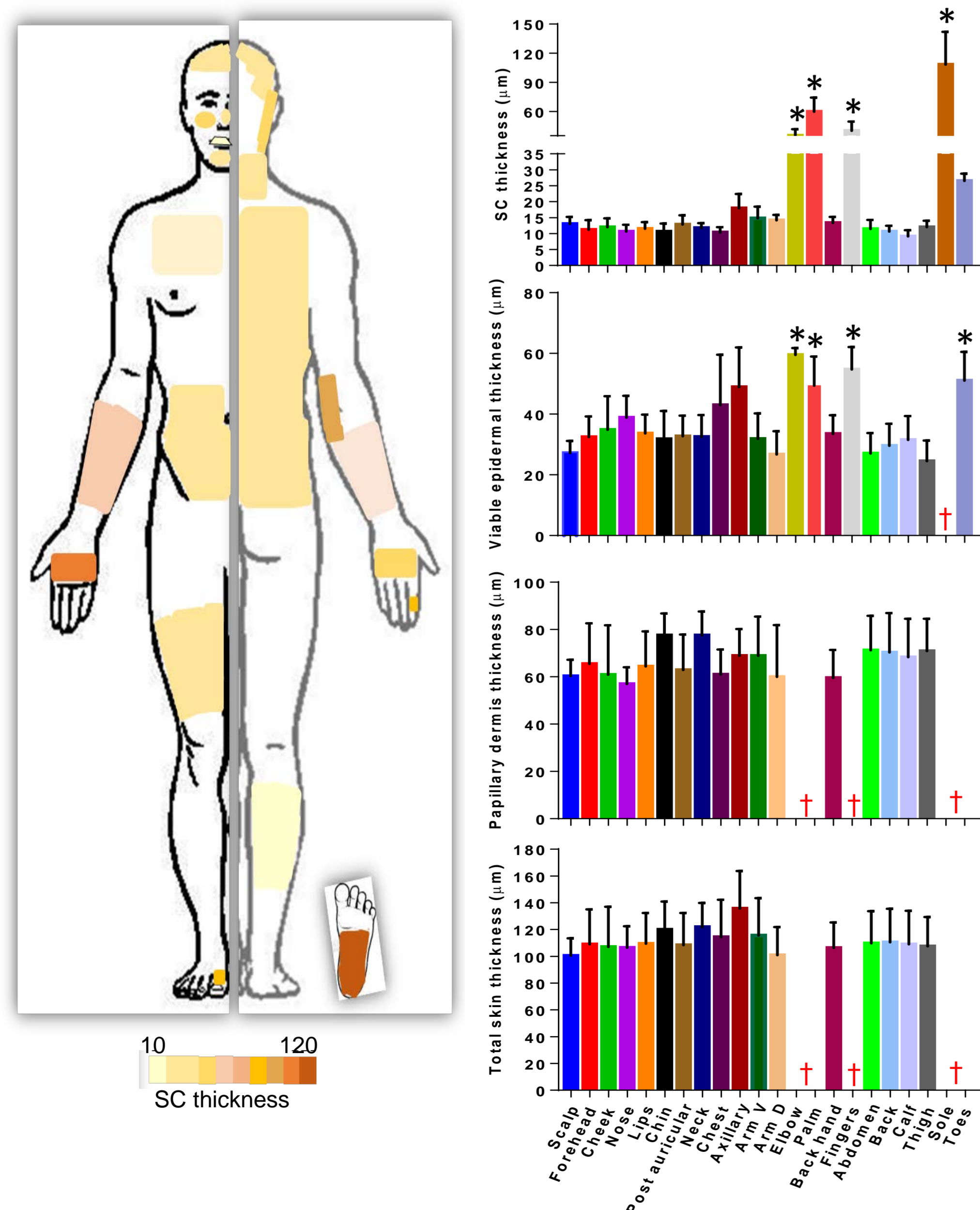


**Figure 1.** Estimated thicknesses of the skin and various layers across the body (\* $p < 0.05$ , compared to abdominal skin). († RCM image unobtainable due to thickness of SC)

**Results 2.** Skin biophysical properties are shown in Table 1. Variations in hair follicle density and sweat gland density across body sites are shown in Fig. 2. Furrows (Fig. 3) are important sites for drug and particle accumulation and their properties may be significant determinants of skin permeation that will be incorporated into the 3D permeation model being developed.

Body Site	SC thickness (h, in $\mu\text{m}$ )	TEWL (g/m <sup>2</sup> /h)	TEWL (g/m <sup>2</sup> /h) Male	TEWL (g/m <sup>2</sup> /h) Female	SH (AU)	D* (=TEWL* $h$ /SH)
1- Scalp	12.6 $\pm$ 2.5	34.8 $\pm$ 4.8	31.4	36.4	3.0 $\pm$ 0.7	142.8
2- Forehead	11.6 $\pm$ 3.0	40.0 $\pm$ 4.4	51.3	34.9	46.6 $\pm$ 8.7	10.2
3- Cheek	12.0 $\pm$ 2.7	37.2 $\pm$ 5.5	49.2	32.5	64.1 $\pm$ 16.4	7.0
4- Chin	10.6 $\pm$ 2.4	66.9 $\pm$ 9.3	83.0	58.9	82.9 $\pm$ 2.0	8.6
5- Nose	10.8 $\pm$ 2.1	62.7 $\pm$ 6.2	63.2	62.4	63.6 $\pm$ 13	10.7
6- Lips	11.9 $\pm$ 2.1	52.7 $\pm$ 6.3	58.0	47.5	57.5 $\pm$ 13	11.0
7- Post-auricular	12.4 $\pm$ 2.9	33.6 $\pm$ 7.0	41.7	30.3	52.4 $\pm$ 16.7	8.0
8- Chest	10.5 $\pm$ 0.5	32.0 $\pm$ 1.7	32.0	31.9	75.0 $\pm$ 11.3	4.5
9- Abdomen	12 $\pm$ 1.0	44.6 $\pm$ 2.5	39.6	49.6	36.2 $\pm$ 15.0	14.8
10- Neck	11.4 $\pm$ 1.4	49.6 $\pm$ 3.2	53.7	45.5	44.5 $\pm$ 11.4	12.8
11- Back	10.7 $\pm$ 1.8	44.9 $\pm$ 3.5	50.2	39.6	61.4 $\pm$ 13.2	7.8
12- Axillary	18.7 $\pm$ 4.4	54.0 $\pm$ 6.2	52.0	56.0	57.7 $\pm$ 18	17.7
13- Elbow	34.7 $\pm$ 6.4	57.5 $\pm$ 9.2	78.7	46.7	32.6 $\pm$ 2.0	62.3
14- Arm V	14.8 $\pm$ 3.6	29.2 $\pm$ 2.3	27.5	30.9	45.5 $\pm$ 7.6	9.7
15- Arm D	14.1 $\pm$ 1.6	22.6 $\pm$ 1.5	26.3	21.2	46.4 $\pm$ 15.0	6.8
16- Palm	59.6 $\pm$ 14.0	29.2 $\pm$ 2.3	27.7	30.8	43.7 $\pm$ 11.0	39.7
17- Back hand	13.8 $\pm$ 1.9	39.7 $\pm$ 3.2	47.4	35.8	45.3 $\pm$ 14.7	12.1
18- Fingers	40.0 $\pm$ 9.5	69.6 $\pm$ 2.3	70	69.5	27.0 $\pm$ 3.3	102.2
19- Thigh	12.3 $\pm$ 2.0	25.7 $\pm$ 2.8	24.7	26.0	47.9 $\pm$ 10.9	6.7
20- Calf	9.2 $\pm$ 1.9	27.4 $\pm$ 3.5	30.9	25.9	40.8 $\pm$ 4.8	6.3
21- Sole	108.3 $\pm$ 23.0	19.0 $\pm$ 3.1	20.0	19.2	78.3 $\pm$ 8.0	26.3
22- Toes	26.5 $\pm$ 2.2	66.6 $\pm$ 8.4	66.0	67.0	35.8 $\pm$ 6.8	50.7

**Table 1.** Skin TEWL, SH and water diffusivity (D\*) at 22 different anatomical sites on the human body

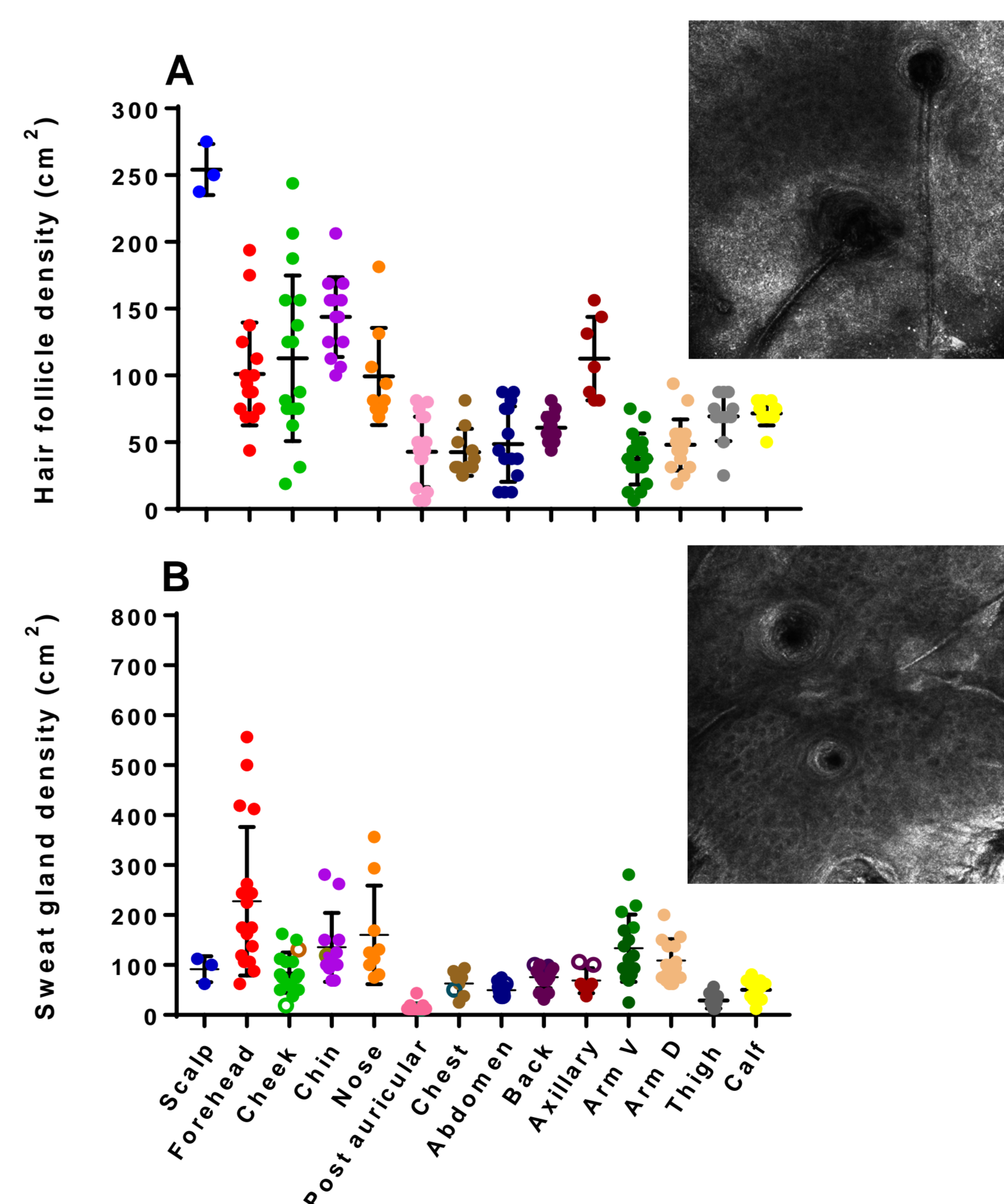


**Figure 2.** A. Hair follicle density and B. sweat gland density at different skin sites (individual values, and mean  $\pm$  SD, count/cm<sup>2</sup>). Also shown are RCM images of hair follicles (A) and sweat glands (B).

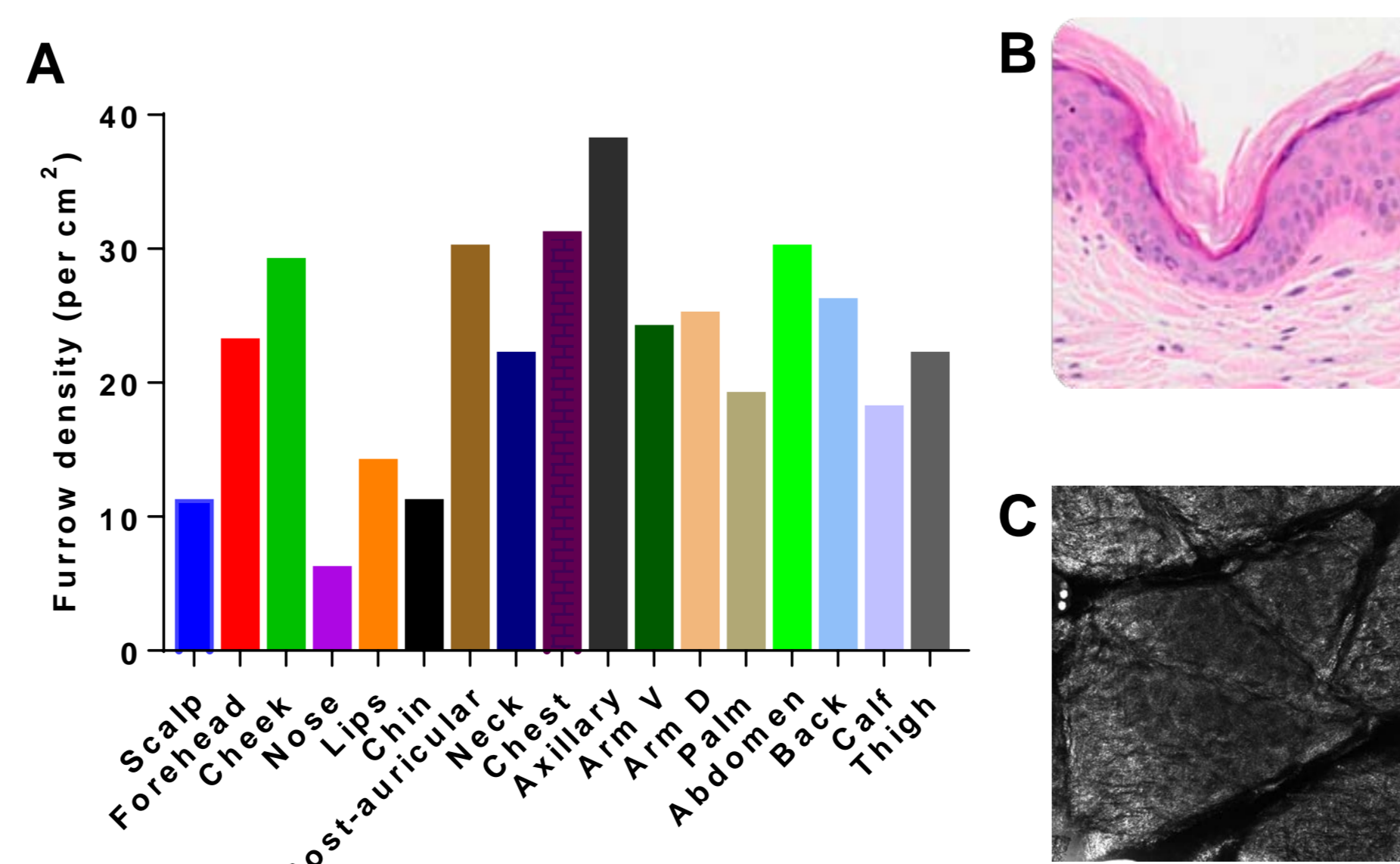


**Figure 3.** A, Skin furrow density (per cm<sup>2</sup>) at different body sites; B, furrow cross-section (H&E stain); C, RCM image of skin furrows

**Results 3.** Based on Fick's First Law, water diffusion through SC can be described by the relationship:  $TEWL = D^* \times SH/h$ , where  $D^*$  is the apparent water diffusivity,  $SH$  is skin hydration and  $h$  is SC thickness [2]. Trends shown in Fig. 4A-C suggest that skin thickness, as well as the densities of hair follicles (HF) and sweat ducts (SD), contribute to water flux through the SC.

A multiple regression equation of the form:  $TEWL = a.SH/h + b.HF + c.SD + d$  gave a predicted:observed  $r^2$  of 0.7406 for the post-auricular site only but poor correlation for all sites combined ( $r^2 = 0.1511$ ). Site variations in skin properties, including diffusivity, may be a factor.

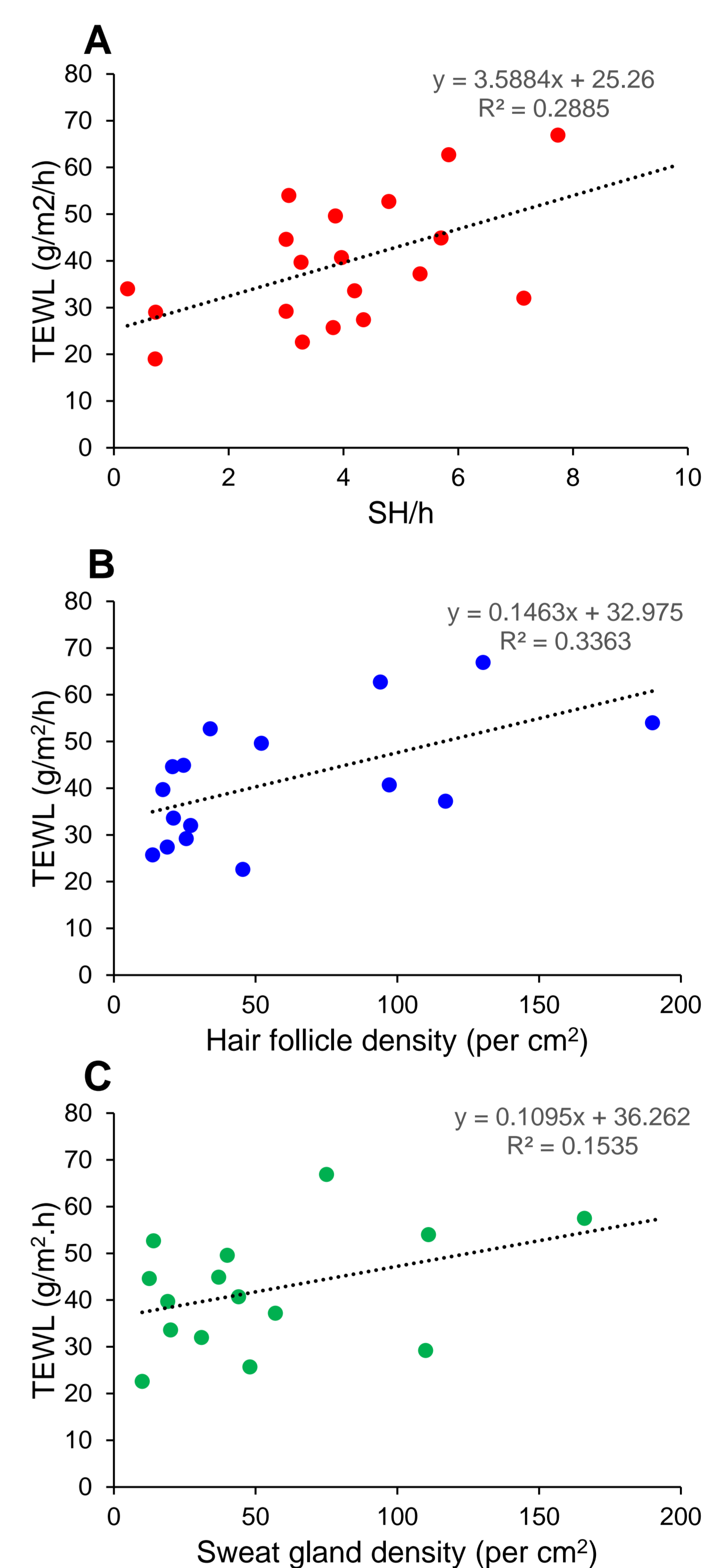


**Figure 4.** Relationships between TEWL and A, SH/h; B, hair follicle density; and C, sweat gland density for different body sites (mean values).

## Conclusions

We have created a database of *in vivo* human skin morphological, physiological and biophysical properties at different anatomical sites, and we have begun exploring interrelationships between the flux of water through skin and the morphology of that skin. We are using these data to develop 3D microscopic and macroscopic models of skin permeation to predict differences in topical bioavailability at a given anatomical site from *in vitro* data obtained at a remote site.

## References

1. Naegel A et al. ADDR 2013;65:191–207.
2. Kalia YN et al. Biophys J 1996;71:2692-700.

## Acknowledgment

MR acknowledges the support of the Australian National Health & Medical Research Council for grants 1107356 and Program Grant APP1055176.